

Sensitivity of Detecting Trabecular Bone Loss using In-Vivo Micro-MRI-based Biomechanics

Wenli Sun¹, Chamith Rajapakse¹, and Felix W. Wehrli¹

¹Radiology, University of Pennsylvania, Philadelphia, PA, United States

Introduction: Detection of bone's short-term mechanical alterations during disease progression (or regression in response to intervention) is critical for proper management of treatment options. Micro magnetic resonance imaging (μMRI) based finite-element (μFE) modeling at peripheral sites is emerging as an attractive means to capture temporal changes in bone. However, the detection sensitivity of μFE analysis performed on the basis of models generated from 3D images similar to those achievable under *in-vivo* μMRI conditions has not previously been investigated. The purpose of this study was to examine whether mechanical implications resulting from a small amounts of bone loss can be reliably detected in the limited spatial resolution and signal-to-noise-ratio (SNR) regime of *in-vivo* μMRI. Toward this goal, we compared the μFE-derived stiffness computed on the basis of “*in-vivo*” μMR images simulated from 3D computer models of trabecular bone (TB) network derived from high-resolution micro-CT (μCT) images of cadaveric bone before and after synthetically mimicking two forms of bone loss: (1) trabecular thinning (TT) via homogeneous erosion and (2) trabecular perforation (TP) via heterogeneous bone loss. The null hypothesis is that there is no difference in pre- and post-bone loss μFE-derived stiffness at *in-vivo* resolution and SNR.

Methods:

Image acquisition: Cadaveric human distal tibiae from 15 donors (4 females and 11 males, aged 55–84 years) had previously been imaged by μCT (μCT 80, Scanco Medical, Switzerland) at 25 μm isotropic voxel size with marrow in situ [1].

Image pre-processing: The processing steps preceding μFE analysis are illustrated in Fig 1. Each high-resolution μCT image was first segmented at a threshold corresponding to the midpoint between the bone and background peaks of the image intensity histogram. Cortical bone was then stripped using an operator-guided program to yield a binary voxel model (i.e. 3D image) of the TB compartment for a 5-mm axial segment.

Bone loss simulation: Two sets of degraded models were created by mimicking bone loss via TT and TP [2]. TT models were generated by iteratively removing bone voxels on trabecular surfaces until the bone volume decreased by volume fractions of 0.5, 1 and 2%. TP was performed by creating pits 50 μm in diameter centered on random trabecular surface voxels until bone volume was decreased by the same three fractions.

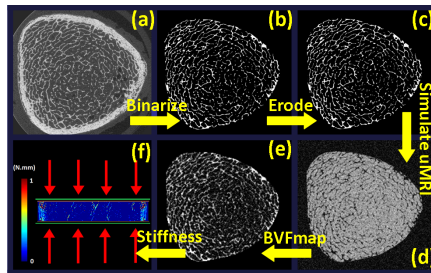
Simulation of μMRI: To generate simulated μMR images at *in-vivo* imaging resolution currently achievable at peripheral scan locations contrast of the 3D binary images was first inverted so that bone appears hypo-intense as in MRI. The images were then converted to k-space by fast Fourier transform (FFT). To emulate the μMRI acquisition process at 150-μm isotropic voxel size (now achievable *in-vivo* imaging) [3], k-space data were low-pass filtered with a 3D rectangular function and apodized to avoid ringing artifacts. Further, to mimic signal-to-noise ratios (SNR) obtainable in typical *in-vivo* μMRI scan times, Gaussian distributed noise was superimposed to the resulting complex images yielding magnitude “μMR” images with SNR=20, 15, and 10. The grayscale μMR image intensities were linearly scaled from 0 to 100%, with pure bone and pure “marrow” having minimum and maximum values, respectively. Subsequently, contrast of the resulting images was inverted to generate bone-volume fraction (BVF) maps for stiffness analyzing, in which bone is hyper-intense.

FE-model generation: First, each bone voxel in the BVF map was directly converted to a hexahedral finite element with dimensions equal to the voxel size. Bone tissue was assumed to be isotropic and linearly elastic. Each element's Young's modulus (YM) was set linearly proportional to BVF at that voxel using $YM = 15 \text{ GPa} \times \text{BVF}$ while Poisson's ratio was kept constant at 0.3 [4].

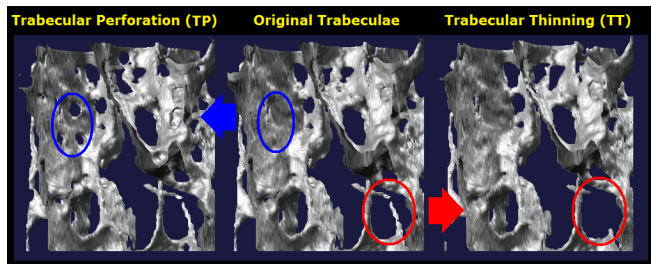
Computation of stiffness: To estimate axial stiffness, compressive loading was simulated along bone's longitudinal axis by applying 1% strain to all nodes in the proximal face of the μFE model while keeping those in the distal face constrained. Axial stiffness was obtained as the ratio of the stress on the proximal face to the applied strain.

Results: Under simulated *in-vivo* μMR conditions, detectable change in BVF was always lower than the applied bone loss (data points below the line of identity in Figure 3). Detectable change in FE-derived stiffness was greater than that for BVF in all cases (data points above the line of identity in Figure 3). TT yielded slightly greater detectable effect size for stiffness than under TP, while for BVF the opposite was true. (3) The detectable effect size decreased with decreasing SNR as expected, while a bone loss as small as 0.5% at the lowest SNR value tested was detectable. Data also show that decreased SNR causes the apparent BVF to increase, which is in agreement with previous reports [2].

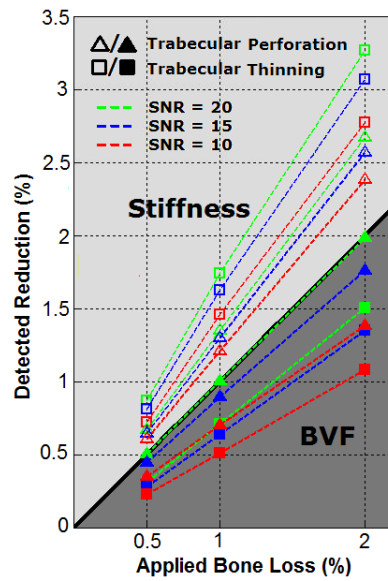
Conclusion: The data suggest that mechanical implications caused by subtle changes in TB typical of short-term bone loss in patients are detectable via FE analysis under imaging conditions now achievable by *in-vivo* μMRI.



← Figure 1: Illustration of processing sequence: Axial views of a μCT image (a); TB compartment segmented (b); bone loss simulated (c); simulated to μMRI resolution and superimposed with noise (d); inverted to BVF map (e); axial stiffness computed via FEA (f).



← Figure 2: 3D renderings of a small TB region before and after simulated bone loss via TT and TP. TT (red) and TP (blue).



← Figure 3: Detected changes in BVF and FE-derived stiffness (y-axis) corresponding to 0.5%, 1%, and 2% simulated bone loss (x-axis) from trabecular perforation and thinning at SNR values of 20, 15, and 10. Solid black line is the line of identity. The detected changes were highly significant ($p < 0.00005$) for all cases.

References: [1] Rajapakse, Bone, 2010; [2] Li, Med Phys, 2008; [3] Wald, JMRI, 2010; [4] Rajapakse, ASBMR, 2008;

Acknowledgements: NIH RO1 AR 55647 and K25 AR 060283.